Cyst Infection of Intraductal Papillary Mucinous Neoplasms of the Pancreas: Management of a Rare Complication

Report of 2 Cases

Kenji Watanabe, MD, Hidenori Karasaki, MD, PhD,† Yusuke Mizukami, MD, PhD,‡ Toru Kawamoto, MD, PhD,§ Toru Kono, MD, PhD,|| Koji Imai, MD, PhD,* Takahiro Einama, MD, PhD,* Masahiko Taniguchi, MD, PhD,* Yutaka Kohgo, MD, PhD,§ and Hiroyuki Furukawa, MD, PhD**

Abstract: The purpose of this study was to describe the cyst infection of intraductal papillary mucinous neoplasm in 2 patients. The patients were 62- and 74-year-old men. The initial symptom was acute febrile abdominal pain. Laboratory tests revealed severe infection (C-reactive protein concentrations were 23.3 μg/mL in patient 1 and 22.3 μg/mL in patient 2) and multilocular cystic masses (the diameters were 70 mm in patient 1 and 50 mm in patient 2) at the pancreatic head that involved peripancreatic vessels were demonstrated by computed tomography. Laboratory and radiographic findings were markedly improved by endoscopic transpapillary drainage. The enteric bacteria were detected in the drainage specimens. Curative resection was achieved, and histological findings indicated a carcinoma in situ in patient 1 and an invasive carcinoma in patient 2. Neither hyperamylasemia nor histological fat necrosis, frequently observed in acute pancreatitis, was evident. Both patients were free from recurrence after surgery (17 months in patient 1, and 18 months in patient 2). Cyst infection is an unknown complication of intraductal papillary mucinous neoplasm. Transpapillary drainage is highly recommended as an initial intervention. It is difficult to distinguish between cyst infection and unresectable invasive carcinoma with imaging modalities; however, surgical intervention after drainage may contribute to long-term survival.

Key Words: intraductal papillary mucinous neoplasms, cyst infection, transpapillary drainage

(*Pancreas* 2014;43: 478–481)

Intraductal papillary mucinous neoplasm (IPMN) of the pancreas is a common pancreatic tumor that is characterized by the intraductal and papillary proliferation of neoplastic cells and the production of thick fluid.[1] Since it was originally described in the 1980s by Ohashi et al,[2] a large number of studies have been performed to establish the etiology of this tumor. Intraductal papillary mucinous neoplasms are classified as main-duct or branch-duct types depending on the location of the lesion.[3] They are also subdivided into 4 types (gastric, intestinal, pancreaticobiliary, and oncocytic) based on morphological features.[4] Although a number of studies have investigated the use of imaging modalities or cytogenetic analysis of tissue and fluid samples obtained by endoscopy to estimate tumor grade, IPMN staging is still subject to debate.[5,6] In general, surgical intervention is highly recommended for patients with main duct tumors or large branch-duct tumors with mural nodules.[7] In addition, patients who have IPMN-related symptoms are generally considered to be candidates for surgical resection.[8] Acute pancreatitis (AP), caused by large amounts of mucin, has been recognized as a major complication of IPMN, and the incidence of AP in the largest surgical series published to date varied from 12% to 67%.[9] Sendai guidelines recommend surgical resection in patients with branch-duct IPMN and clinical symptoms, including AP.[3] In contrast with the relatively high frequency of AP coexistent with IPMNs, reports of cyst infection associated with IPMN are rare. We report our experience with 2 patients with IPMN who developed sepsis due to cyst infection, which is a rare but notable complication of IPMN. Herein, we discuss the diagnosis, initial treatment, and management strategy for IPMN associated with cyst infection, which may represent an unknown complication of IPMN.

PATIENT 1

A 62-year-old man was admitted to a local clinic complaining of epigastralgia with fever. He was treated by administration of antibiotics without relief of symptoms. The patient was then referred to our hospital for further intervention. He had been abusing alcohol (360 mL of distilled spirits per day) for 40 years and had diabetes mellitus, hypertension, and benign prostatic hypertrophy. There was no history of AP. Blood tests revealed a marked inflammatory response: 18,660 white blood cells/μL and 23.3 μg/mL C-reactive protein (CRP). All of the tumor markers that we examined were within reference range. Serum pancreatic amylase values were within normal limits, but elastase 1 was elevated to 640 ng/dL. A computed tomography (CT) scan revealed a multilocular cystic tumor 70 mm in diameter at the head and the uncinate process of the pancreas. The tumor involved peripancreatic vessels, including the celiac artery, the superior mesenteric artery, and the portal vein (PV) (Figs. 1A, B, and D). Transpapillary nasopancreatic drainage tube, 7F in diameter, was inserted to cyst immediately after admission to our hospital. Cannulation was not difficult, because the orifice of the duodenal papilla was markedly dilated by copious amounts of mucin (Fig. 1G). The patient defervesced 3 days after drainage. The amount of drainage fluid was 170 mL at day 1 and decreased to 32 mL at day 3 after procedure. The drainage tube was removed at 9 days after drainage. *Enterococcus faecalis* and *Escherichia coli* were detected in the pus discharge. Cytological examination of the drained fluid revealed mucin-producing papillary clusters with mild atypia and positive immunoreactivity for MUC2 and NUC5AC. Both laboratory and imaging findings

From the *Division of Gastroenterological and General Surgery, Department of Surgery, Asahikawa Medical University; †Department of Surgery, Social Work Association Furano Hospital; ‡Center for Clinical and Biomedical Research, Sapporo Higashi Tokushukai Hospital; §Division of Gastroenterology and Hematology/Oncology, Department of Medicine, Asahikawa Medical University; and ||Advanced Surgery Center, Sapporo Higashi Tokushukai Hospital, Hokkaido, Japan.

Received for publication March 9, 2013; accepted August 9, 2013.

Reprints: Hidenori Karasaki, MD, PhD, Department of Surgery, Social Work Association Furano Hospital, 1-30 Sumiyoshityo, Furano, Hokkaido 076-8765, Japan (e-mail: hide.karasaki@gmail.com).

The authors declare no conflict of interest.

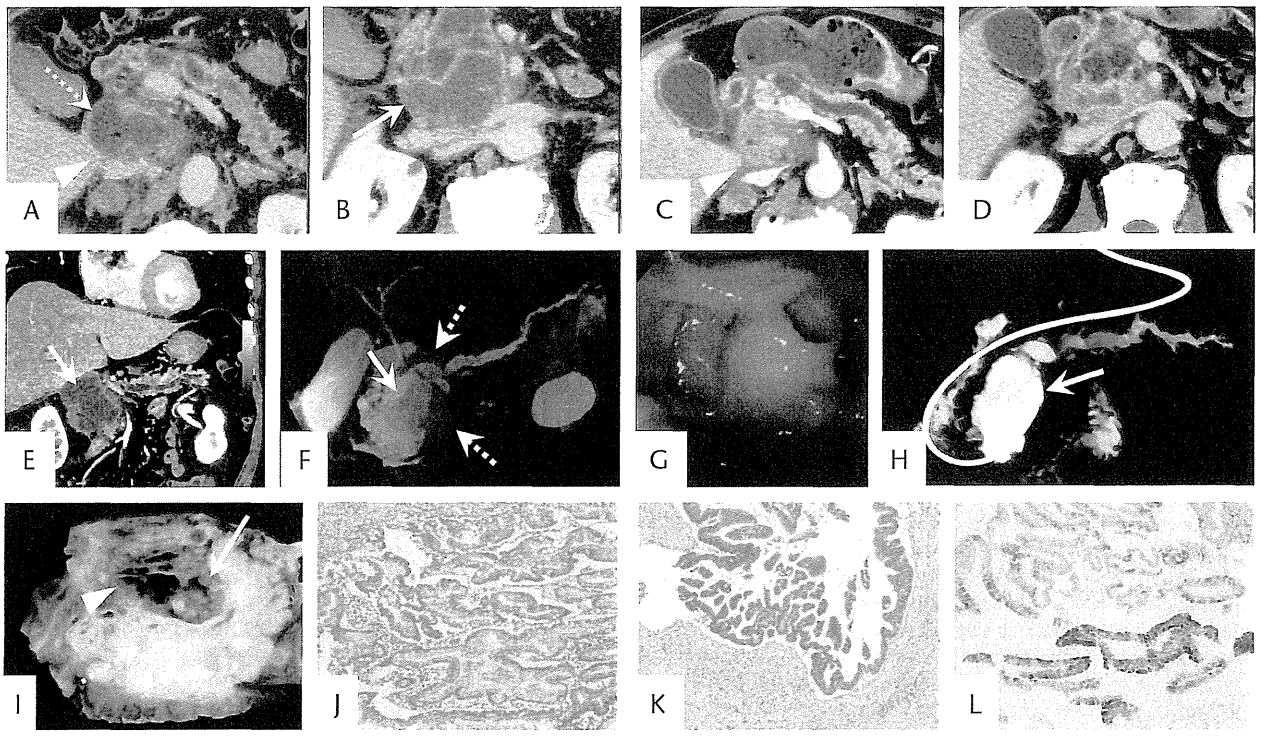

FIGURE 1. Imaging findings and resected specimen of patient 1. Computed tomography images of patient 1 before (A and B) and after (C and D) transpapillary cyst drainage are shown in the top panel; cystic lesions of the pancreas head composed of ventral (arrow) and dorsal part (dashed arrow). Both lesions shrunk markedly after drainage. The interface between dorsal lesion and IVC was poorly demarcated, even after drainage (arrow head). Postdrainage images are demonstrated in the middle panel; multiplanar reconstruction coronal CT (E), magnetic resonance cholangiopancreatography (F), and endoscopic retrograde cholangiopancreatography (G and H) findings are shown. Arrow indicates ventral cyst, and dashed arrow shows dorsal one. The orifice of duodenal papilla (G) was dilated by a copious amount of mucin. The catheter was easily placed transpapillary into the ventral cyst (arrow) connecting to main pancreatic duct (H). Macroscopic (I) and pathological (J, K, and L) findings in the bottom panel. A cystic lesion connected to the main pancreatic duct (arrowhead) at the ventral side of the specimen was observed. The major part of the tumor (J: solid arrow in I) was composed of moderately dysplastic papillary epithelium. The tall columnar tumor cells were characterized by abundant apical mucin with basally located nuclei. Moderate amounts of eosinophilic cytoplasm were revealed by hematoxylin-eosin (H&E) staining. The dorsal part of the pancreas head (dashed arrow) was replaced by yellowish-white sclerotic tissue. This hard area was composed mostly of granulation tissue and partly of high-grade dysplastic columnar epithelium with pseudostratified nuclei and basophilic cytoplasm (K: H&E staining). Neoplastic cells at the inflamed site were diffusely positive for MUC2 staining (L).

were improved by endoscopic drainage, and pylorus-preserving pancreaticoduodenectomy was performed (Figs. 1C, D). During the surgical intervention, adhesive solid tissue between the pancreatic head and inferior vena cava (IVC) was partly preserved, assuming that the mass may have been inflammatory in nature. However, pathological tests revealed that the tumor was composed mostly of gastric-type IPMN with moderate dysplasia, and part of the solid component was intestinal-type IPMN (carcinoma in situ) with massive inflammatory infiltrates (Figs. 1I-L). The patient was free from recurrence 17 months after surgery.

PATIENT 2

A 74-year-old man was admitted to our hospital complaining of abdominal pain and fever. He had a history of alcohol consumption (180 mL of distilled spirits per day) for 33 years, as well as a medical history of AP that had been treated conservatively when he was in his 60s. Laboratory tests at admission revealed severe inflammation (25,960 white blood cells/μL and 22.3 μg/mL CRP) and liver dysfunction (117 IU/L aspartate aminotransferase and 99 IU/L alanine aminotransferase). Hyperamylasemia was not observed. Tumor markers, including carcinoembryonic antigen and CA-19-9, were within reference range. Computed tomography scans showed a multilocular cystic tumor with a diameter of 50 mm located at the pancreatic head, and dilatation of the main pancreatic duct was observed (Figs. 2A, B). Several antibiotics were administered intravenously and nasobiliary transpapillary pancreatic duct drainage tube, 7F in diameter, was inserted to the main pancreatic duct, but his general status was not improved. Therefore, the drainage tube was replaced to drain cyst (branched duct) on the sixth day of hospitalization. This was easily performed, as in patient 1. The patient defervesced immediately after cyst drainage. The amount of drainage fluid was 3 to 20 mL a day. Because slightly high CRP value was prolonged even after defervescence, the tube had been placed for 17 days. *Corynebacterium striatum* was detected in the drained fluid. Atypical regenerative cell clusters in the inflamed background were identified by cytological examination. Macrophages engulfing mucin with positive immunoreactivity for MUC2 and MUC5AC were observed. Symptoms and the inflammatory findings revealed by imaging were significantly improved by endoscopic drainage (Figs. 2C, D). The tumor, with heterogeneous enhancement by intravenous contrast material, persisted after drainage in the pancreatic head; therefore, pylorus-preserving pancreaticoduodenectomy was carried out.

During surgical resection, severe sclerosis/fibrosis of soft tissue in the peripancreatic area was observed, which made it

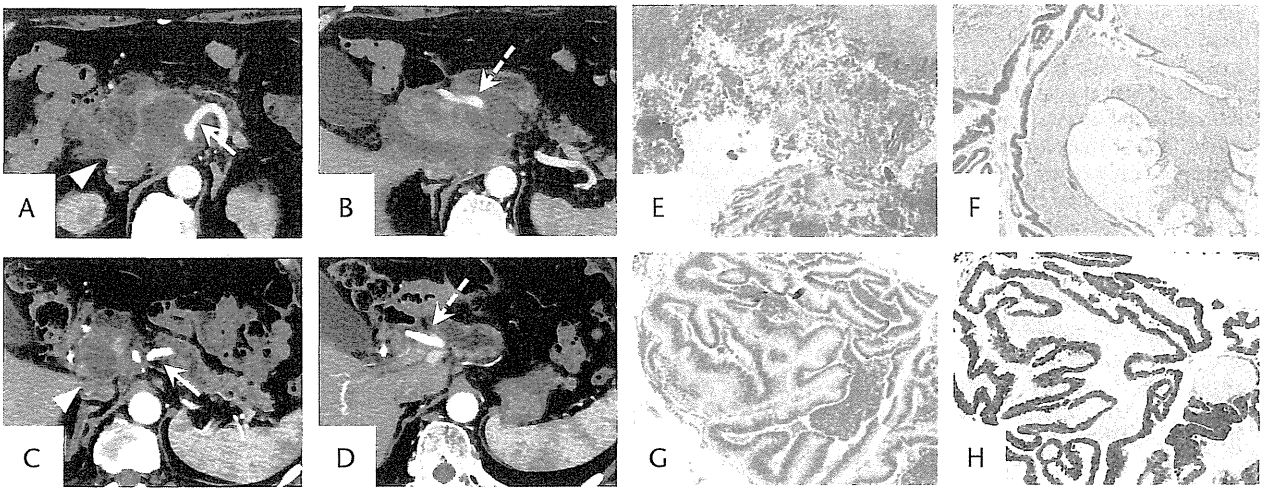

FIGURE 2. Imaging findings and resected specimen of patient 2. Computed tomography scan of patient 2 before (A and B) and after (C and D) transpapillary cyst drainage. A multilocular cystic lesion involving the SPA (solid arrow) and the common hepatic artery (dashed arrow) was observed at the pancreas head. The arteries are clearly separated from the tumor in the postdrainage images. The poorly demarcated boundary between the tumor and IVC was also visualized better following drainage (arrowhead). The cystic lesion was partly lined by papillary proliferating epithelium, and clots of neoplastic cells and necrotic debris were observed in the cavity (E: H&E staining). Severe inflammatory infiltrates were observed in the thickening wall. Invasive tubular adenocarcinoma was observed within the cyst wall (F: H&E staining). The neoplastic epithelium in the branch duct formed tall papillae with columnar cells with pseudostratified nuclei and basophilic cytoplasm (G: H&E staining). The neoplastic cells displayed diffuse MUC2 immunoreactivity (H).

difficult to detach the PV from the tumor; therefore, the PV was excised and reconstructed by external iliac vein graft. The common hepatic artery and the splenic artery (SPA) were preserved, although they were somewhat involved in the indurated tissue periphery of the tumor. Pathologically, the tumor was an adenocarcinoma arising from intestinal-type IPMN with an invasive component on the cyst wall (Figs. 2E-H). The indurated tissue on the surgical margin was an inflammatory change, and it did not appear to contain tumor cells. The patient received adjuvant chemotherapy with gemcitabine and was free from recurrence 18 months after the surgical intervention.

DISCUSSION

Although a growing number of patients are being diagnosed with IPMN of the pancreas, little is known about IPMN with cyst infection. To our knowledge, no previously published reports of the natural history of IPMN have specifically mentioned this rare complication, and there are a few reports concerning this condition as proceedings in Japanese. At Asahikawa Medical University Hospital, we observed only 2 cases of IPMN with cyst infection out of 70 patients who underwent resection to treat IPMN between 1994 and 2012. Acute pancreatitis is one of the major complications of IPMN.[10,11] Pancreatitis associated with IPMN is generally not severe, and it can sometimes recur without any treatment for IPMN. In contrast, in our patients, cyst infection of IPMNs displayed symptoms associated with sepsis and uncharacterized findings on imaging modalities, which prompted us to recognize it as a clinical category independent of the AP more commonly associated with IPMN.

The symptoms associated with cyst infection began with abdominal pain and fever in our patients. Although severe inflammatory reactions can be identified by blood chemistry examinations, pancreatic hyperenzymemia was not evident; both patients had normal serum amylase levels, and the serum elastase 1 level was only slightly greater than the reference range in 1 patient.

Computed tomography imaging was informative; although it was significantly modified by severe inflammation, scans still revealed the typical morphology of IPMN. Evidence of IPMN was more clearly demonstrated after endoscopic drainage. The tumor mass appeared to involve large vessels and their tributaries around the pancreas; however, it should be noted that this does not always indicate an unresectable and highly invasive tumor. Therefore, images collected before drainage need to be carefully interpreted. Typical findings associated with AP, such as edematous changes of the pancreatic parenchyma and peripancreatic fluid collection, were absent,[12] indicating that the cystic lesions observed in our patients were not due to a complication of acute necrotizing pancreatitis.

Histopathological analyses revealed neoplastic cells with typical IPMN phenotypes, accompanied by necrotic tissue with abundant inflammatory infiltrates in the mass (Fig. 2E). The cyst wall was lined at least partly with viable tumor cells, which distinguished these lesions from pseudocysts of the pancreas. Granulation was evident in the walls of the cysts, where aggressive inflammatory cell infiltration was observed. These histological findings were in accordance with the fluid and solid components revealed by CT scan. It should be noted that very little of edema, hemorrhage, and fat necrosis commonly seen in AP were observed.

The effectiveness of endoscopic drainage to treat infected pancreatic pseudocyst was reported previously.[13] This relatively noninvasive procedure was also effective in our patients, and we recommend it as an initial treatment for cyst infection of IPMNs. In addition to removing the infected fluid, endoscopic drainage also allowed for definitive cytological and pathological diagnosis and provided samples for bacterial culture so that we could determine the appropriate antibiotics for treatment. Because of the enteric bacteria present in the drainage specimens from both patients, we considered that the infection route was most likely retrograde, which is common in AP.[14] The laboratory and imaging findings improved remarkably after drainage, and these changes were important not only for differentiating

IPMN with cyst infection from invasive carcinoma, but also for determining whether the patients could be treated with surgical intervention. The predrainage imaging findings of IPMN with cyst infection appeared serious enough that we were unsure whether surgical intervention was appropriate; however, as we found after drainage, most of the "tumor tissue" was actually composed of severely inflamed tissue. Because of the difficulty in predicting tumor margins based on radiographic findings, whole mass resection may be unavoidable. In the present report, the IVC, which was covered by sclerosing connective tissue surrounding the tumor, was also preserved in the first patient (Fig. 1A). The common hepatic artery and SPA, which were thought to be involved by the tumor before drainage, could be preserved in the second patient (Figs. 2A, B). Pathological assessment indicated that the sclerosing tissue was inflammatory granuloma and that the surgical margins were histologically free of invasion by carcinoma cells.

Recent advances in endoscopic procedure have provided options with regard to drainage routes, but the transpapillary route, rather than the transluminal route through the stomach/duodenum, should be considered first, because it is less invasive.[13] Cannulation into the abscess via Vater papilla was feasible in our patients, because the pancreatic duct and the orifices of the papillae were widely dilated because of copious mucin produced by the IPMNs (Figs. 1F, G). Indeed, in both cases, endoscopic drainage was technically easy. However, in patients in whom it would be difficult to reach the infected cyst(s) via the transpapillary route, endoscopic ultrasound-guided drainage via the transluminal route should be considered as an alternative. In general, once infection of neoplastic cysts occurs, it is difficult for antibiotics administration alone to eliminate severe inflammation; therefore, immediate endoscopic abscess drainage should be considered.

Surgical resection of IPMN lesions with cyst infection is highly recommended after sufficient abscess drainage at the earliest possible opportunity for the following reasons. First, cyst infection can relapse easily; the closed space formed by occlusion between the dilated branch and the main pancreatic duct due to the tumor itself or to the presence of viscous mucin is conducive to pathogenesis; therefore, infections may occur repeatedly after endoscopic drainage alone. In patients with AP associated with IPMN, the intestinal subtype has been considered particularly high risk because of copious viscous mucin production.[11] In our report, the tumor was positive for MUC2 staining in the first patient. Although in the second patient the tumor was mostly MUC2 negative, the lesion at the infected area was of the MUC2-positive intestinal type. A retrospective histological review of tumors previously resected in our hospital indicated that 14 patients were intestinal-type out of 17 patients who had symptoms associated with AP (82.4%). Therefore, MUC2-positive IPMN may tend to cause mucin-associated symptoms. Tissue fibrosis and granulation in the cyst wall may be caused by repeated infection; therefore, these lesions should be treated not only by endoscopic drainage, but also by resection to prevent recurrence of infection. Second, IPMN with cyst infection may also indicate a high-grade tumor, as demonstrated by the association between the existence of symptoms and the malignancy of IPMNs.[8] The rate of AP in IPMN patients has been proposed to correlate with malignant potential.[11] It should be noted that both of our patients had tumors that were histologically malignant; moreover, the second patient developed invasive carcinoma.

In conclusion, cyst infection in IPMN should be considered as a potential complication. Transpapillary abscess drainage is effective as an initial treatment, and surgical resection soon after drainage is highly recommended, because of the risk of recurrent infection and the high probability of malignancy.

REFERENCES

1. Adsay NV, Kloppel G, Fukushima N, et al. Intraductalneoplasms of the pancreas. In: Bosman F, Carneiro F, Hruban RH, et al, eds. *WHO Classification of Tumours of the Digestive System*. 4th ed. Lyon, France: IRAC; 2010:304–313.
2. Ohashi K, Murakami Y, Maruyama M, et al. Four cases of mucous secreting pancreatic cancer. [in Japanese, with English abstract]. *Prog Digest Endosc*. 1982;20:348–351.
3. Tanaka M, Chari S, Adsay V, et al. International consensus guidelines for management of intraductal papillary mucinous neoplasms and mucinous cystic neoplasms of the pancreas. *Pancreatology*. 2006;6:17–32.
4. Furukawa T, Kloppel G, Volkan Adsay N, et al. Classification of types of intraductal papillary-mucinous neoplasm of the pancreas: a consensus study. *Virchows Arch*. 2005;447:794–799.
5. Schmidt CM, White PB, Waters JA, et al. Intraductal papillary mucinous neoplasms: predictors of malignant and invasive pathology. *Ann Surg*. 2007;246:644–651; discussion 51–54.
6. Kawai M, Uchiyama K, Tani M, et al. Clinicopathological features of malignant intraductal papillary mucinous tumors of the pancreas: the differential diagnosis from benign entities. *Arch Surg*. 2004;139:188–192.
7. Salvia R, Fernandez-del Castillo C, Bassi C, et al. Main-duct intraductal papillary mucinous neoplasms of the pancreas: clinical predictors of malignancy and long-term survival following resection. *Ann Surg*. 2004;239:678–685; discussion 85–87.
8. Sugiyama M, Izumisato Y, Abe N, et al. Predictive factors for malignancy in intraductal papillary-mucinous tumours of the pancreas. *Br J Surg*. 2003;90:1244–1249.
9. McGrath K, Slivka A. Diagnosis and management of intraductal papillary mucinous neoplasia. *Nat Clin Pract Gastroenterol Hepatol*. 2005;2:316–322.
10. Pelletier AL, Hammel P, Rebours V, et al. Acute pancreatitis in patients operated on for intraductal papillary mucinous neoplasms of the pancreas: frequency, severity, and clinicopathologic correlations. *Pancreas*. 2010;39:658–661.
11. Tsutsumi K, Ohtsuka T, Oda Y, et al. A history of acute pancreatitis in intraductal papillary mucinous neoplasms of the pancreas is a potential predictive factor for malignant papillary subtype. *Pancreatology*. 2010;10:707–712.
12. Banks PA, Freeman ML. Practice guidelines in acute pancreatitis. *Am J Gastroenterol*. 2006;101:2379–2400.
13. Lerch MM, Stier A, Wahnschaffe U, et al. Pancreatic pseudocysts: observation, endoscopic drainage, or resection? *Deutsch Arzteblatt Int*. 2009;106:614–621.
14. Luiten EJ, Hop WC, Endtz HP, et al. Prognostic importance of gram-negative intestinal colonization preceding pancreatic infection in severe acute pancreatitis. Results of a controlled clinical trial of selective decontamination. *Intensive Care Med*. 1998;24:438–445.

Hindawi Publishing Corporation
Gastroenterology Research and Practice
Volume 2013, Article ID 384057, 8 pages
http://dx.doi.org/10.1155/2013/384057

Hindawi

Research Article

Preventive Effect of TU-100 on a Type-2 Model of Colitis in Mice: Possible Involvement of Enhancing Adrenomedullin in Intestinal Epithelial Cells

Atsushi Kaneko,[1] Toru Kono,[2,3] Naoko Miura,[1] Naoko Tsuchiya,[1] and Masahiro Yamamoto[1]

[1] *Tsumura Research Laboratories, Tsumura & Co., 3586 Yoshiwara, Ami-machi, Inashiki-gun, Ibaraki 300-1192, Japan*
[2] *Faculty of Pharmaceutical Sciences, Hokkaido University, Sapporo 060-0812, Japan*
[3] *Center for Clinical and Biomedical Research, Sapporo Higashi Tokushukai Hospital, Sapporo 065-0033, Japan*

Correspondence should be addressed to Atsushi Kaneko; kaneko_atsushi@mail.tsumura.co.jp

Received 20 August 2013; Revised 1 October 2013; Accepted 7 October 2013

Academic Editor: Bjørn Moum

Purpose. Crohn's disease (CD) and ulcerative colitis (UC), the two major forms of inflammatory bowel disease (IBD), have histopathologically and immunologically different characteristics. We previously reported that a traditional Japanese medicine, daikenchuto (TU-100), ameliorated a trinitrobenzenesulfonic acid- (TNBS-) induced type-1 model colitis exhibiting histopathological features of CD through adrenomedullin (ADM) enhancement. Our current aims were to examine whether TU-100 ameliorates a type-2 model colitis that histologically resembles UC and identify the active ingredients. *Methods.* TU-100 was administered orally to mice with oxazolone- (OXN-) induced type-2 model colitis. The morbidity was evaluated by body weight loss and the macroscopic score of colonic lesions. ADM was quantified using an EIA kit. *Results.* TU-100 prevented weight loss and colon ulceration. ADM production by intestinal epithelial cells was increased by TU-100 addition. Screening to identify active ingredients showed that [6]-shogaol and hydroxy α-sanshool enhanced ADM production. *Conclusions.* TU-100 exerted a protective effect in OXN-induced type-2 model colitis, indicating that TU-100 may be a beneficial agent for treatment of UC.

1. Introduction

Inflammatory bowel diseases (IBD), including Crohn's disease (CD) and ulcerative colitis (UC), are chronic progressive and destructive disorders of the gastrointestinal tract, characterized by inflammation associated with uncontrolled innate and adaptive immunity against normal bowel constituents like commensal bacteria and various microbial products [1]. Meanwhile, an etiologic role for splanchnic blood flow in IBD has been relatively neglected. The gastrointestinal epithelium is anatomically positioned to provide a selective barrier between the anaerobic lumen and lamina propria, which is supported by a complex vasculature. This important barrier is affected by reduced blood flow and resultant tissue hypoxia, particularly in sites of active inflammation in individuals with IBD [2]. Daikenchuto (TU-100), a pharmaceutical-grade traditional Japanese (*kampo*) medicine, has been widely used for the treatment of various gastrointestinal disorders including postoperative ileus [3]. TU-100 has been integrated into the modern medical care system in Japan as a prescription drug. We recently clarified the mechanism by which TU-100 increases intestinal blood flow [4]. TU-100 activates transient receptor potential ankyrin 1 (TRPA1) expressed on intestinal epithelial cells, followed by release of the vasodilator peptide adrenomedullin (ADM). The vasodilatory effect of TU-100 has been shown in clinical [5] and experimental studies [4, 6–9]. ADM was initially identified as a vasodilator and is thought to be the most potent endogenous vasodilatory peptide found in the body [10, 11]. Other effects of ADM include augmentation of the tolerance of cells to oxidative stress and hypoxic injury, angiogenesis, anti-inflammation, and antibiotic activity. Moreover, several reports indicate that administration of ADM prevented development of colitis in experimental IBD models [12–18].

CD and UC have immunologically different pathobiologies. The responding T cells in CD and UC exhibit T helper cell (Th) 1 and 2 phenotypes, respectively. Among various experimental colitis models, hapten-induced colitis in rodents caused by intrarectal administration of trinitrobenzene sulfonic acid (TNBS) and oxazolone (OXN) is thought of as a type-1 colitis animal model resembling CD and a type-2 model resembling UC, respectively. Therefore, therapeutic strategies for IBD include the use and development of various immunomodulating agents as the most powerful and promising methods.

We previously reported that TU-100 ameliorated TNBS-induced type-1 colitis in mice via enhancement of intestinal release of ADM [19]. Considering that the effect of TU-100 is related to endogenous ADM in the intestines, we hypothesized that TU-100 would be effective in treatment of other types of colitis with different immunological properties. The aim of the present study was to clarify whether TU-100 has a beneficial effect on an OXN-induced type-2 model colitis.

2. Materials and Methods

2.1. Test Samples. Daikenchuto extract in the form of a dried powder was obtained from Tsumura & Co. (Tokyo, Japan), which manufactures it as an aqueous extract containing processed ginger, ginseng radix, and Japanese pepper in the ratio of 5 : 3 : 2. The extract yielded 12.5% by weight. TU-100 was prepared by mixing daikenchuto extract powder and maltose syrup powder (Tsumura & Co.) at a ratio of 1 : 8. Hydroxy α-sanshool was extracted from Japanese pepper at Tsumura & Co. with a purity of 97.9%. [6]-Gingerol, [6]-shogaol, ginsenoside Rb1, ginsenoside Rg1, ginsenoside Rd, and maltose were purchased from Wako Pure Chemical Industries, Ltd. (Osaka, Japan). Xanthoxylin was purchased from Tokyo Chemical Industry (Tokyo, Japan).

2.2. Animals. Five-week-old male C57BL/6CrSlc mice were purchased from Japan SLC (Shizuoka, Japan). The animals were allowed free access to water and standard laboratory food and housed at a temperature of 23 ± 2°C, relative humidity of 55 ± 10%, and a 12 h light : 12 h dark cycle, with lights on from 07:00 to 19:00 h daily. All experimental procedures were performed according to the "Guidelines for the care and use of laboratory animals" of Tsumura & Co. Ethical approval of the experimental procedures used in this study was obtained from the Laboratory Animal Committee of Tsumura & Co.

2.3. OXN-Induced Colitis. Colitis was induced following the methods described by Hyun et al. [20] with slight modification. Briefly, under pentobarbital anesthesia, 100 μL of 1% OXN (4-ethoxymethylene-2-phenyl-2-oxazolin-5-one, Sigma-Aldrich, St. Louis, MO) dissolved in a mixture of four parts acetone to one part olive oil was applied to the shaved abdominal skin of mice. One week later, 100 μL of 50% ethanol solution with or without 1% OXN was instilled rectally under anesthesia with pentobarbital and atropine (Sigma-Aldrich, 3 mg/kg, i.p.). The mice were held in a vertical position (head down) for 30 seconds and then put back into their cages. After 4 d, the mice were sacrificed, the colon was dissected, and macroscopic colonic lesions were graded on a scale from 0 to 11 based on criteria reflecting hemorrhage (0-1), edema (0-1), stricture (0-1), ulceration (0-1), fecal blood (0-1), mucus (0-1), diarrhea (0-1), erythema (0, absent; 1, less than 1 cm; and 2, more than 1 cm), and adhesion (0, absent; 1, moderate; and 2, severe). This animal test rarely causes death, but one mouse among 16 colitis control mice died during this experiment. We evaluated the disease activity score excluding the dead mouse.

TU-100 in distilled water was given orally at 900 mg/kg to colitis mice several hours, 1, 2, and 3 d after OXN instillation. The dose of TU-100 given to mice was based on previous publications on experimental TU-100 studies, which reported the beneficial effects of TU-100 related to clinical efficacy. Further, the dose used in the present study was expected to produce blood concentrations of the major ingredients in mice similar to those in humans (data not shown).

2.4. ADM Production Test. Rat small intestine epithelial cell lines IEC-6 and IEC-18 were obtained from DS Pharmaceuticals (Osaka, Japan) and grown in DMEM supplemented with 10% heat-inactivated fetal bovine serum (FBS), 2 mmol/L L-glutamine, 100 U/mL penicillin, 100 μg/mL streptomycin, and 10 mmol/L HEPES. IEC-6 or IEC-18 cells between the 30th and 37th passage were plated in 96-well flat-bottom microtiter plates at 1×10^4 cells/well in DMEM supplemented with the same additives described above, allowed to settle overnight, and then culture fluids were replaced with fresh medium containing 3% FBS and test sample. TU-100 was added to cultures at final concentrations of 270, 900, and 2700 μg/mL after being passed through a 0.45 μm filter. Cells were incubated for 24 h, and ADM in the culture fluids was quantified using an enzyme immunoassay kit specific for rat ADM according to the instructions provided by the manufacturer (Phoenix Pharmaceuticals, Burlingame, CA). The lowest level of detection for ADM was 10 pg/mL.

2.5. Cell Growth Test. IEC-6 cells were treated with the test sample as described above. After culture fluids were removed for ADM quantification, cell growth activities were measured using an XTT reduction assay kit (Biological Industries, Beit Haemek, Israel) under the manufacturer's instructions. Optical density at 465 nm was measured by subtracting the reference absorbance at 630 nm. The optical density of the medium-only wells was in a range of 0.07 to 0.10.

2.6. Cytokine Induction Tests. Spleen mononuclear cells were isolated from normal C57BL/6CrSlc mice. Erythrocytes were removed from a spleen cell suspension by hypotonic lysis in ammonium chloride and potassium chloride buffer. The cells were seeded in 96-well flat-bottom microtiter plates (5×10^5 cells/mL) in RPMI 1640 medium supplemented with 10% FBS, 100 units/mL penicillin and 100 μg/mL streptomycin, 10 mmol/L HEPES, and 50 μmol/L 2-mercaptoethanol and stimulated with *E. coli*-derived lipopolysaccharide (LPS,

1 μg/mL, Sigma-Aldrich) for 2 d or an antibody against mouse CD3 (anti-CD3, clone 145-2C11, 1 μg/mL; BD Biosciences, San Jose, CA) for 1 d. ADM was added to cultures at 0.01, 0.1, or 1 μmol/L. Culture supernatants were collected and then stored at −80°C until the cytokine assay. Cytokines were measured using a Bio-Plex Pro mouse cytokine assay panel (Bio-Rad Laboratories, Inc., Hercules, CA) according to the manufacturer's instructions. IL-17A and TNF-α were measured using conventional ELISA assay reagents produced by BD Biosciences and R&D Biosystems (Minneapolis, MN), respectively. The lowest levels of detection were 9.36 (IL-1β), 0.86 (IL-2), 0.28 (IL-4), 2.77 (IL-5), 0.21 (IL-6), 0.87 (IL-10), 5.06 (IL-12p70), 11.55 (IL-13), 11.09 (GM-CSF), 15.54 (IFN-γ), 37.14 (MCP-1), and 4.11 (IL-17A and TNF-α).

2.7. Statistical Analysis. All values are expressed as the mean ± SEM. Statistical significance was evaluated by one- or two-way analysis of variance (ANOVA), and a probability of less than 0.05 was considered significant at Student's t-test or Dunnett's test.

3. Results

3.1. Ameliorating Effect of TU-100 in OXN-Induced Colitis. The OXN-treated mice developed rapid-onset colitis marked by weight loss, diarrhea, and bloody stool. The body weight of the OXN-treated group decreased transiently from day 1 to day 2 after OXN instillation. Oral administration of TU-100 at 900 mg/kg, the dosage for treatment of the TNBS-induced colitis model [19], resulted in a marked prevention of ulcerative colitis, as well as a reduction in the loss of body weight (Figure 1).

3.2. ADM Enhancement by TU-100 Addition. Next, we investigated the effect of TU-100 on cultures of IEC-6 and IEC-18 cells; the former were used in our previous studies [4, 7, 19], and Kishikawa et al. used the latter for demonstration of LPS-induced ADM synthesis in intestinal epithelial cells [21]. As shown in Figure 2, TU-100 increased ADM production by both IEC-6 cells and IEC-18 cells in a concentration-dependent matter. Table 1 shows the results of screening the major ingredients of TU-100 for their stimulatory effect on ADM in IEC-6. [6]-Shogaol, an ingredient of processed ginger, and hydroxy α-sanshool, an ingredient of Japanese pepper, have been shown to stimulate ADM from IEC-6 cells. Neither active ingredient showed a significant inhibition on cell growth following their additions. Essentially the same results were obtained for the experiment using IEC-18 cells (data not shown).

3.3. Inhibition of Proinflammatory Cytokines by ADM Addition. ADM is known to have suppressive effects on proinflammatory cytokines such as TNF-α in various inflammation models [15]. Therefore, we examined the effects of ADM on cytokine production by murine spleen cells (Table 2). In the anti-CD3 stimulation assay, ADM significantly suppressed the production of IL-13, GM-CSF, IFNγ, and TNF-α, but not IL-1β, IL-2, IL-4, IL-5, IL-6, IL-10, IL-12p70, or IL-17A, while ADM augmented IL-2 production only at the highest concentration. Furthermore, ADM inhibited the LPS-induced production of GM-CSF, IFNγ, MCP-1, and TNF-α, but not IL-2, IL-6, IL-10, or IL-12p70. These data show that ADM is not an immunomodulator that deflects either the Th1 or Th2 response as far as the profile of cytokine productions was examined.

4. Discussion

We examined the large intestines of TU-100-treated mice by macroscopic and histological observations, but found no change compared with those of nontreated mice (data not shown). The histological features of the colon in OXN-treated mice were as previously reported [20]. Superficial inflammation was characterized by epithelial cell loss and/or regenerative epithelium, depletion of goblet cells, inflammatory cell infiltration composed mainly of neutrophils and eosinophils, edema formation, hemorrhage, vascular dilatations, and occasionally crypt abscesses. In the present study, we observed that OXN-treated mice exhibited typical characteristics of OXN-induced colitis such as hemorrhage, edema, ulceration, diarrhea, and erythema. Compared with the colitis control group, mice in the TU-100-treated colitis group exhibited remarkable alleviation of these colitis processes.

CD and UC have traditionally been distinguished by patterns of helper T-cell dysfunction. Lamina propria cells from patients with CD overproduce cytokines associated with a Th1 response, such as IL-12 and IFN-γ. In contrast, cells from patients with UC overproduce cytokines associated with the Th2 response, such as IL-5 and IL-13. Studies of mouse models of mucosal inflammation (e.g., type-1 TNBS- and type-2 OXN-induced colitis) have provided further evidence that activities of Th1 and Th2 cells mediate the pathogenesis of CD and UC, respectively [1]. Therefore, the effects of immunomodulating agents on CD, UC, and their disease models have been shown to be different, sometimes even contradictory. For example, a certain anti-TNF monoclonal antibody has been reported to be effective in TNBS-induced colitis but not in OXN-induced colitis [22]. Further, infection with Helminth parasites ameliorates TNBS-induced colitis but exaggerates OXN-induced colitis via eosinophilia and elevated IL-5 [23].

However, distinguishing CD from UC based on overproduction of Th1 and Th2 cytokines is an oversimplification of a complex immunological response. Much of the inflammatory pathology originally believed to be mediated by Th1 cells and IL-12 has been found to be mediated by a subset of T cells, Th17 cells, which produce the IL-17 family members IL-21 and IL-22 at sites of inflammation and require the IL-12 family member IL-23 as a growth factor [24]. Adding to the complexity, Th1, Th2, and Th17 cells have both pro- and anti-inflammatory properties in various types of mucosal inflammation [25].

Further, there are commonalities underpinning their pathogenesis. The pathogenesis of IBD includes a complex interaction between innate and adaptive immune cells, local

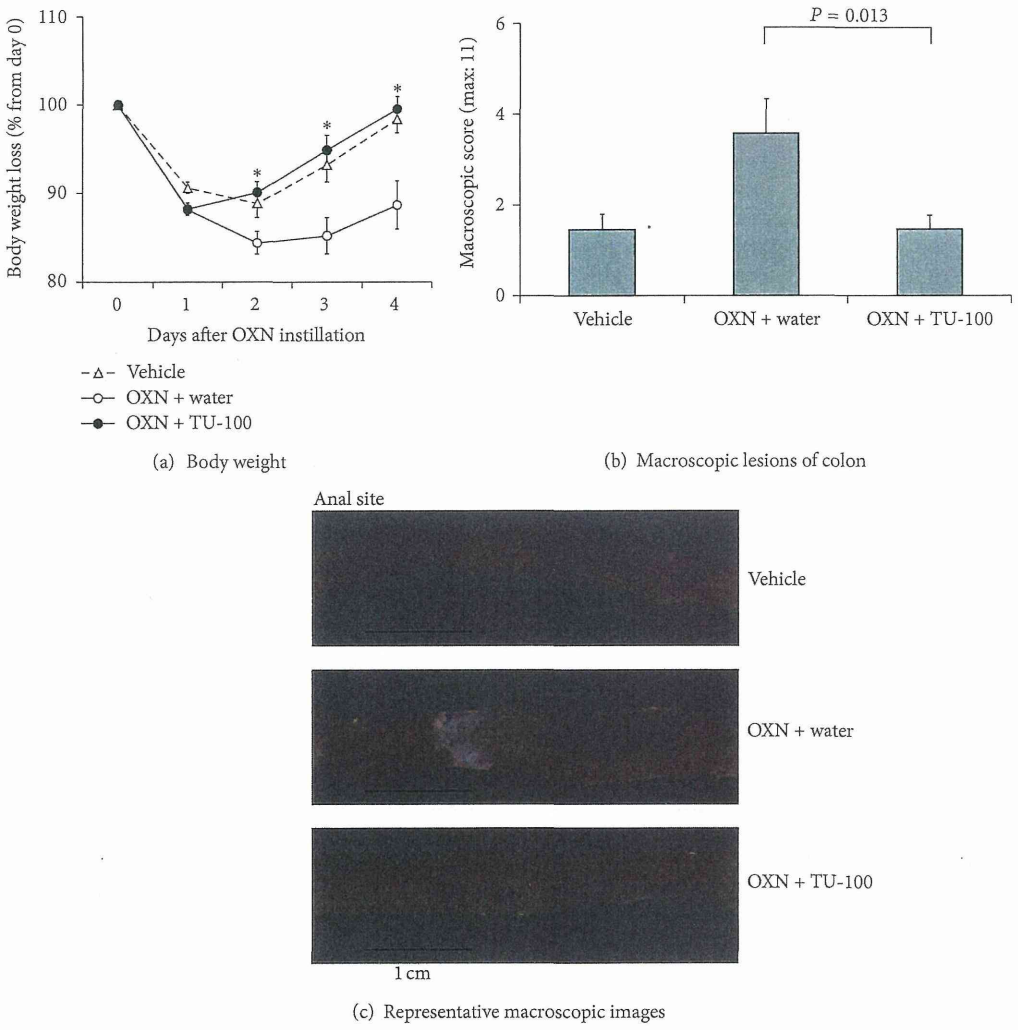

FIGURE 1: Effects of TU-100 on body weight and macroscopic colon lesions in OXN-induced colitis. Mice were presensitized with oxazolone (OXN, 1 mg/100 μL applied to skin), and then OXN (1 mg/100 μL) or vehicle, 50% ethanol, was instilled intrarectally (i.r.). TU-100 (900 mg/kg) was given orally to mice several hours, 1, 2, and 3 days after OXN instillation, and mice were sacrificed 4 days after OXN instillation. Body weight changes after OXN instillation (a), and macroscopic scores of colon lesions (b) are shown. Representative macroscopic images of each group are shown (c). Vehicle: 50% ethanol i.r. + water p.o., $N = 11$, OXN + water: OXN i.r. + water p.o., $N = 14$, OXN + TU-100: OXN i.r. + TU-100 p.o., $N = 15$, $^*P < 0.05$ versus colitis control by Student's t-test.

immune modulators and cytokines, intestinal vasculature, nutritional factors, and enteric microbiota. Therefore, intervention by dietary management and probiotic ingestion are still clinically effective therapeutic options for CD and UC [26–28], though they have yet to attain an acceptable evidence-based status. In addition, a variety of agents such as FK506-entrapped nanoparticles [29], viral and nonviral NF-κB decoys [30, 31], blockade of CD30-CD30L interaction [32], IL-25 [33], leptin [34], and a plant-derived compound [35] have been shown to ameliorate both colitis models. TU-100 showed ameliorating effects on TNBS-induced colitis in previous studies [7, 19] and OXN-induced colitis in the present study. TU-100 is, therefore, a candidate for a novel therapeutic agent for both CD and UC. Though the clinical efficacy of TU-100 in IBD is still unclear, accumulating case reports in Japan suggest the possible efficacy of TU-100 in a wide variety of gastrointestinal disorders including CD and UC. Further, placebo-controlled double blind studies of TU-100 on IBD are now in progress in the US (NCT01388933).

Although the mechanism by which TU-100 exerts its ameliorating effects on OXN-induced colitis remains to be elucidated, it is plausible that the ADM released by TU-100 stimulation plays several roles. As we previously reported, intestinal epithelial cells of the small and large intestines produce much ADM and release it following stimulation of TRPA1 channels expressed on their plasma membranes [4, 7, 19]. There was no difference between the small and large intestines in ADM expression and responses to TU-100 stimulation followed by ADM production. Hydroxy α-sanshool and [6]-shogaol are known to be nonselective

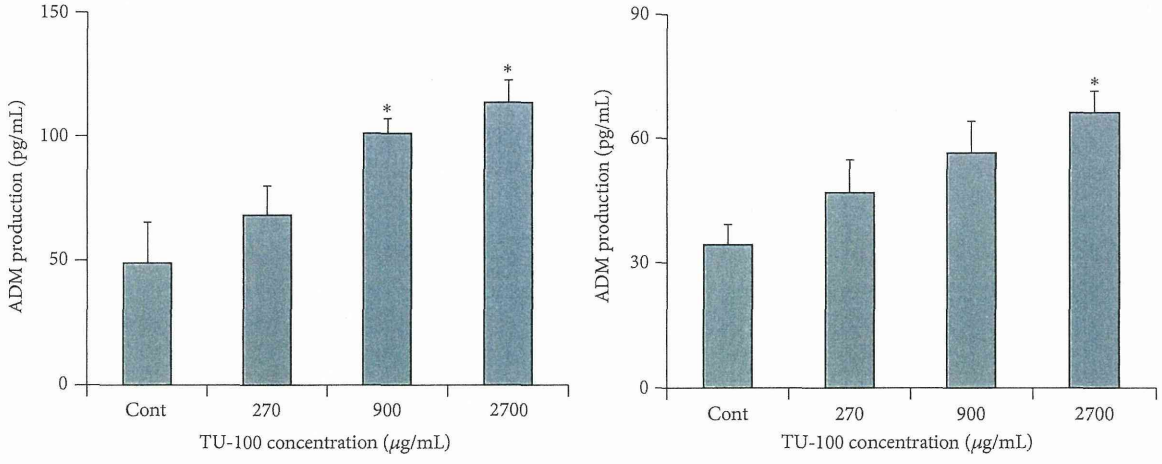

FIGURE 2: Adrenomedullin-enhancing activity of TU-100 in intestinal epithelial cells. Intestinal epithelial cell lines IEC-6 (a) and IEC-18 (b) settled overnight were incubated with the indicated concentrations of TU-100 for 1 day. Adrenomedullin (ADM) in the culture fluid was determined by ADM-specific EIA. $N = 4$ (a), 3 (b). $^*P < 0.05$ versus control by Dunnett test.

TABLE 1: Screening for ingredients that enhance ADM production.

Test sample origin	Ingredient	Concentration (μmol/L)	Growth activity (optical density)	ADM production (pg/mL)
—	Control	—	1.419 ± 0.045	85.3 ± 4.9
Processed ginger	[6]-Gingerol	3	1.429 ± 0.016	99.7 ± 12.4
		30	1.400 ± 0.025	93.0 ± 6.5
	[6]-Shogaol	3	1.504 ± 0.019	100.0 ± 9.3
		30	1.363 ± 0.023	246.3 ± 5.0*
Ginseng radix	Ginsenoside Rb1	3	1.399 ± 0.014	98.0 ± 2.6
		30	1.366 ± 0.047	90.7 ± 9.2
	Ginsenoside Rg1	3	1.393 ± 0.067	89.0 ± 5.1
		30	1.375 ± 0.040	95.7 ± 3.8
	Ginsenoside Rd	3	1.379 ± 0.045	88.3 ± 5.4
		30	1.386 ± 0.026	103.3 ± 12.3
Japanese pepper	Xanthoxylin	3	1.429 ± 0.030	89.3 ± 7.4
		30	1.395 ± 0.012	99.0 ± 12.1
	Hydroxy α-sanshool	3	1.449 ± 0.009	110.3 ± 12.5
		30	1.557 ± 0.013*	120.3 ± 8.8*
		100	1.493 ± 0.043	162.0 ± 1.7*
Maltose syrup	Maltose	30	1.484 ± 0.019	106.7 ± 11.0
		300	1.467 ± 0.031	106.7 ± 11.7

IEC-6 cells were settled overnight and cultured for 1 d with or without the test sample at the indicated concentrations. ADM in the culture fluids was measured by EIA. Cell growth was measured using an XTT reduction assay kit. $N = 3$. $^*P < 0.05$ versus control by Dunnett test.

agonists of TRPA1 channels [36]. Therefore, exposure of intestinal epithelial cells to them results in increases of ADM production and release.

The representative Th2 cytokine IL-13 is expressed abundantly in the inflamed intestinal mucosa and reported to be profoundly involved in development of OXN-induced colitis [37]. Our studies examining the regulatory effects of ADM on cytokine induction showed that ADM inhibited IL-13 produced by anti-CD3 stimulation. Overall, ADM has demonstrated anticolitis effects in TNBS- [15, 18], DSS- [12, 16, 17], and acetic-acid-induced [14] colitis models. The suppressant effect of TU-100 on mucosal damage [19], mucosal ischemia [7], and especially TNF-α production was shown in TNBS-induced colitis in an ADM-dependent manner. It should be noted that ADM potently decreased TNF-α production induced by both anti-CD3 and LPS in the present

Table 2: Effects of adrenomedullin on cytokine induction due to anti-CD3 or LPS stimulation.

(a) Anti-CD3 stimulation

Cytokine	ADM (μmol/L)			
	Control	0.01	0.1	1
IL-1β	29 ± 5	24 ± 3	24 ± 3	33 ± 9
IL-2	448 ± 37	460 ± 27	475 ± 31	595 ± 28*
IL-4	54 ± 3	50 ± 2	47 ± 3	50 ± 1
IL-5	2 ± 0	4 ± 1	2 ± 0	3 ± 1
IL-6	91 ± 4	94 ± 8	94 ± 4	109 ± 4
IL-10	12 ± 1	14 ± 0	11 ± 1	12 ± 1
IL-12p70	20 ± 3	17 ± 4	19 ± 3	19 ± 5
IL-13	140 ± 4	126 ± 12	90 ± 7*	91 ± 3*
IL-17A	103 ± 2	102 ± 6	106 ± 12	102 ± 12
GM-CSF	81 ± 5	75 ± 1	57 ± 2*	54 ± 4*
IFN-γ	3,821 ± 161	3,177 ± 313	2,110 ± 39*	1,959 ± 117*
TNF-α	16 ± 0	14 ± 0	10 ± 1*	8 ± 1*

(b) LPS stimulation

Cytokine	ADM (μmol/L)			
	Control	0.01	0.1	1
IL-6	326 ± 9	338 ± 4	350 ± 17	328 ± 13
IL-10	551 ± 50	551 ± 10	523 ± 30	472 ± 12
IL-12p70	22 ± 5	15 ± 5	10 ± 3	16 ± 3
GM-CSF	31 ± 3	27 ± 3	19 ± 2*	18 ± 2*
IFN-γ	44 ± 15	36 ± 12	N.D.	N.D.
MCP-1	262 ± 15	260 ± 24	161 ± 12*	149 ± 28*
TNF-α	81 ± 3	72 ± 4	37 ± 3*	28 ± 2*

Murine spleen cells were stimulated with 1 μg/mL anti-CD3 for 1 d (a) or 1 μg/mL LPS for 2 d (b). Adrenomedullin (ADM) was added to culture medium at the indicated concentrations. Cytokines were measured using a Bio-Plex mouse cytokine multiplex kit. Measurements of IL-17A and TNF-α were performed by conventional ELISA. Cytokine productions with no stimulus were 9.9 ± 1.6 in IL-2, 1.6 ± 0.2 in IL-6, 1.7 ± 0.2 in IL-10, and below the detection limit for the others. N = 3-4. *$P < 0.05$ versus control by Dunnett test.

study. It is reported that ADM upregulates intracellular cAMP, which activates protein kinase A and CREB pathways, resulting in suppression of transcriptional factors, such as NF-kB, that are critical for induction of proinflammatory cytokines [38]. TNF-α has been known to be an extraordinarily important pathogenic factor in CD and UC, and an anti-TNF-α antibody is an effective treatment option for patients with moderate to severe UC with an inadequate response to conventional glucocorticoid treatment [39] as well as CD patients. Only IL-2 production by CD3-stimulated cells was significantly enhanced by addition of 1 μmol/L ADM. IL-2 is a pleiotropic cytokine produced by naïve T cells and activated Th1 cells and was identified originally as a growth factor for various lymphocytes [40]. T cells increase the beta subunit CD122 of IL-2 receptors following activation to form a high affinity IL-2 receptor with alpha subunit CD25. ADM evidently suppressed T cell activation as far as focusing on the other cytokines downregulation and may decrease consumption of native T cell-derived IL-2.

In considering the anticolitis effect of TU-100 through enhancement of ADM production, not only the anti-immune action but also the multifunctional effects of ADM should be noted. Our previous study showed that TU-100 improved microvascular circulation at inflammatory ischemia sites of colitis via endogenous ADM release [7]. ADM is reported to protect against inflammatory hypoxia-induced damage of the intestinal epithelium through fine tuning of hypoxia-induced factor stabilization in a DSS-induced colitis model [17]. Moreover, ADM enhanced expression of the epithelial intercellular junctions such as tight and adherence junctions, followed by improvement of hyperactivation and hyperpermeability of the intestinal epithelium in a DSS-induced colitis model [12]. Antimicrobial effects of ADM are known [41] and may affect the development of colitis.

Considering the results shown in Table 2, [6]-shogaol and hydroxy α-sanshool are suggested to be the major active ingredients of TU-100 for stimulation of ADM release and presumably the main ingredients of TU-100 that express anticolitis effects. Ginger-derived various ingredients like gingerols and shogaols are known to inhibit cyclooxygenase enzymatic activity and expression and block intracellular signals induced by inflammatory factors [42, 43]. In addition, ginseng-derived ginsenosides are also reported to exhibit various biological effects like anti-inflammation and antiapoptosis [44]. TU-100, therefore, has many active ingredients and should be considered a multitarget agent, although we focused on ingredients to increase ADM in this study.